Journal Pre-proof

Effects of contaminant metal ions on precipitation recovery of rare earth elements using oxalic acid

Wencai Zhang, Aaron Noble, Bin Ji, Qi Li

PII: S1002-0721(20)30460-9

DOI: https://doi.org/10.1016/j.jre.2020.11.008

Reference: JRE 894

To appear in: *Journal of Rare Earths*

Received Date: 3 September 2020

Revised Date: 8 November 2020

Accepted Date: 11 November 2020

Please cite this article as: Zhang W, Noble A, Ji B, Li Q, Effects of contaminant metal ions on precipitation recovery of rare earth elements using oxalic acid, *Journal of Rare Earths*, https://doi.org/10.1016/j.jre.2020.11.008.

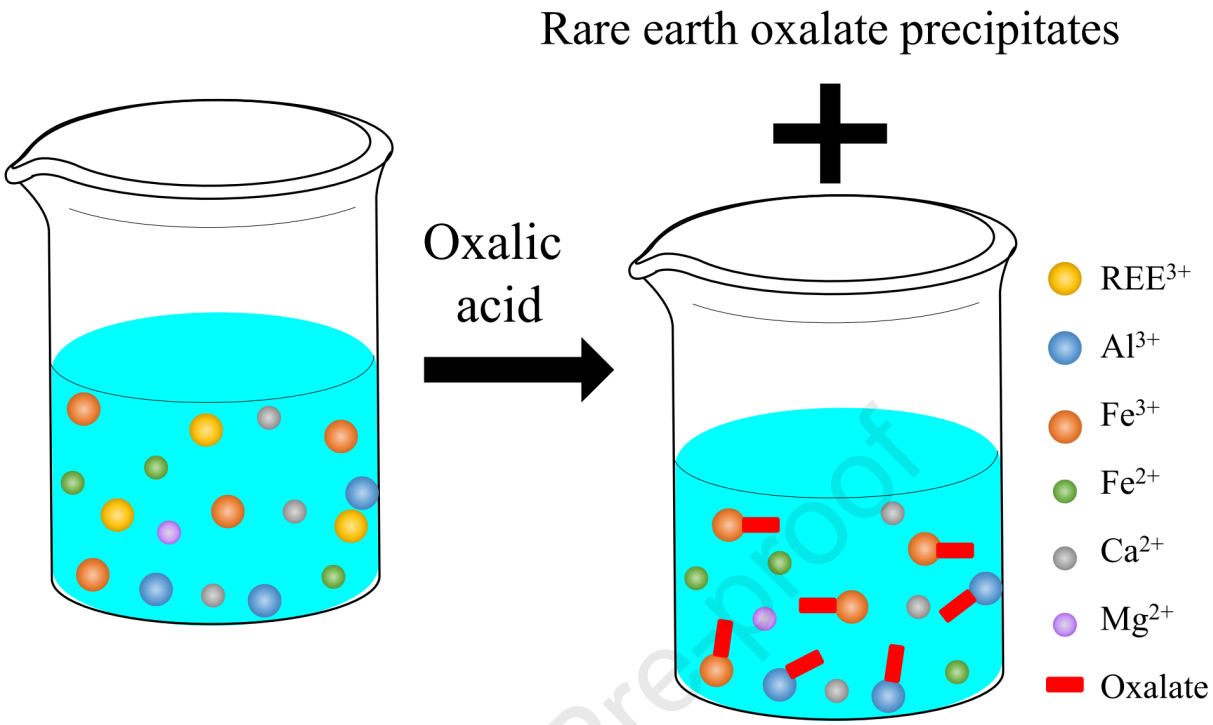

During the selective precipitation process of rare earths using oxalic acid, consumption of the precipitant is largely increased by trivalent metal ions, such as Al^{3+} and Fe^{3+}, while divalent metal ions impose minor impact.

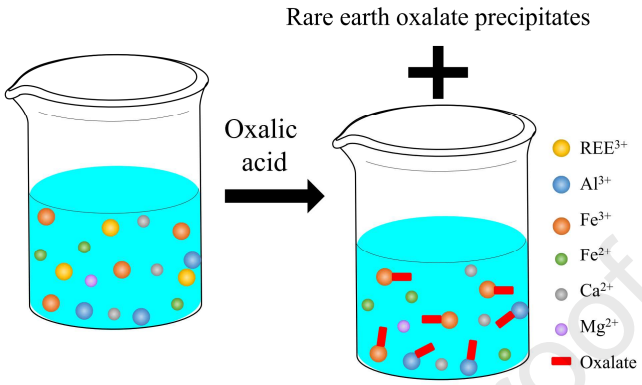

Effects of contaminant metal ions on precipitation recovery of rare earth elements using oxalic acid

Wencai Zhang*, Aaron Noble, Bin Ji, Qi Li

Department of Mining and Minerals Engineering, Virginia Polytechnic Institute and State University, Blacksburg, Virginia 24061, USA

Abstract: Solution equilibrium calculations were performed in this study to understand the impact of contaminant metal ions on the precipitation efficiency of selected rare earth elements (Ce^{3+}, Nd^{3+}, and Y^{3+}) using oxalic acid as a precipitant. Trivalent metal ions, Al^{3+} and Fe^{3+}, were found to considerably affect the precipitation efficiency of REEs. When Al^{3+} and Fe^{3+} concentrations were increased by 1×10^{-4} mol/L, in order to achieve an acceptable cerium recovery of 93% from solutions containing 1×10^{-4} mol/L Ce^{3+}, oxalate dosage needed to increase by 1.2×10^{-4} and 1.68×10^{-4} mol/L, respectively. Such great impacts on the required oxalate dosage were also observed for Nd^{3+} and Y^{3+}, which indicates that oxalic acid consumption and cost will be largely increased when the trivalent metal ions exist in REE-concentrated solutions. Effects of the divalent metal ions on the oxalate dosage is minimal. Furthermore, solution equilibrium calculation results showed that the precipitation of Fe^{3+} and Ca^{2+} (e.g., hematite and $Ca(C_2O_4)\cdot H_2O_{(s)}$) likely occurs during the oxalate precipitation of REEs at relatively high pH (e.g., pH 2.5), which will reduce rare earth oxalate product purity. In addition to the metal ions, anionic species, especially SO_4^{2-}, were also found to negatively affect the precipitation recovery of REEs. For example, when 0.1 mol/L SO_4^{2-} occurs in a solution containing 1×10^{-4} mol/L Ce^{3+} and 4×10^{-4} mol/L oxalate, the pH needed to be elevated from 2.0 to 3.3 to achieve the acceptable recovery. Overall, findings from this study provide guidance for the obtainment of high-purity rare earth products from solutions containing a considerable amount of contaminant metal ions by means of oxalic acid precipitation.

Keywords: Rare earth elements; Oxalic acid; Precipitation; Contaminant metal ions

*Corresponding author: W.C. Zhang

Email address: wencaizhang@vt.edu

Telephone Number: +1-(540) 231-8110

1. Introduction

Rare earth elements (REEs) are essential raw materials for modern technology with strategic importance in both civilian and defense applications. In the conventional supply chain, REEs are produced from ore resources, including monazite, bastnaesite, and xenotime, as well as from ion-adsorbed clays [1]. Commercially-viable deposits of these minerals are quite scarce, and future technology development, particularly for permanent magnets and electric vehicles, is expected to intensify demand for REEs. Given this increased supply risk, the criticality of REEs has been recently codified by many international agencies and national governments [2,3], and considerable public and private investment has addressed the development of processes to recover REEs from alternative resources. Data from the technical literature has included processes to recover REEs from spent permanent REE magnets, spent nickel metal-hydride batteries, waste phosphors, red mud, coal-based materials (e.g., coal refuse and coal combustion ash), and phosphate rocks [2,4–12].

In the processing of conventional REE ores, the majority of the associated gangue minerals are rejected through proper pretreatment and physical beneficiation, including gravity, magnetic, electrostatic, and froth flotation separations [13]. The resultant mineral concentrates then undergo hydrometallurgical and/or pyrometallurgical processing, whereby the REEs are transferred from the solid phase into solution for further concentration and purification [14–17]. After adequate enrichment and separation, high-purity rare earth salts are precipitated from a concentrated REE solution in the final processing stages. These rare earth salts can then be further refined to high purity metal or sold as individual RE-compounds. In the solution recovery step, different kinds of precipitant, including oxalic acid, sulfate, carbonate, phosphate, and fluoride, have been used to achieve satisfactory precipitation performance [18–20]. Of these options, oxalic acid is currently recognized as the most effective precipitant, due to the relatively low solubility products of rare earth oxalate precipitates [19].

Since the majority of gangue elements are removed during physical beneficiation, the REE solutions generated from conventional ores tend to have a low concentration of contaminant metal ions relative to that of the REEs. Alternatively, many alternate resources are not amenable to physical cleaning and thus have a high concentration of contaminants, sometimes orders of magnitude higher than that of the REEs [21]. For example, in the case of REE production from phosphate rock, a solution containing 1,447 mg/L of REEs and 28,055 mg/L of calcium was generated by leaching [22]. During solution purification, 81% of the calcium was removed by three stages of scrubbing; however, a considerable amount of calcium still remained in the stripping solution that was ultimately subjected to oxalic acid precipitation. In another case, a pre-concentrated solution containing 72 mg/L REEs, 1,355 mg/L Al, 700 mg/L Mg, and 370 mg/L Ca was generated from an acid coal mine drainage [21]. This solution was directly processed using oxalic acid precipitation to generate a high-purity rare earth product.

Since oxalic acid tends to chelate with many trivalent cations, the dose of oxalic acid needed to fully precipitate the REEs is dependent on both the concentrations of REEs and the other

contaminant metals. For cases similar to those mentioned above, a slight change in the upstream processing operations will necessarily impart a significant change to the elemental profile of the REE-enriched solution. As a result, empirical approaches to techno-economic process optimization are wrought with difficulty, as a new suite of precipitation tests must be conducted each time an upstream process variable changes. Unfortunately, fundamental investigations on the impact of contaminant metal ions in the precipitation recovery of REEs have been rarely reported. Chi and Xu [18] studied this phenomenon by combining laboratory experimental tests and solution equilibrium calculations, however the impact of individual metal ions was not studied. Other studies have only cursorily addressed oxalic acid precipitation, often only reporting a single optimal dose [21,23].

In this study, solution equilibrium calculations were conducted to evaluate the impact of Al^{3+}, Fe^{3+}, Fe^{2+}, Mg^{2+}, and Ca^{2+} on the oxalic acid precipitation recovery of several selected REEs (Ce^{3+}, Nd^{3+}, and Y^{3+}), which represent light, middle, and heavy REEs, respectively. As one of the most abundant REEs, more focus was placed on the precipitation characteristics of Ce^{3+}. Recovery of the REEs was calculated as a function of both pH and contaminant metal ion concentration. Oxalate dosages required to achieve an acceptable recovery of the REEs were then calculated in the presence of contaminant metal ions of varying concentrations. In addition, the impact of several anionic species, including NO_3^-, Cl^-, and SO_4^{2-}, on the precipitation characteristics of the REEs was also investigated. Altogether, this modeling exercise was used to obtain better fundamental understanding on the use of oxalic acid precipitation to recover and purify REEs from solutions with high contaminant metal content.

2. Methods

The precipitation characteristics of selected REEs (Ce^{3+}, Nd^{3+}, and Y^{3+}) using oxalic acid as a precipitant were analyzed through solution equilibrium calculations. The equilibrium reactions and corresponding reaction constants at 25 □ are shown in Table 1. The majority of the reaction constants were selected from the database of Visual MINTEQ 3.1 software. The constants of a few reactions that are not included in the database were obtained from the literature. Solubility products of cerium sulfate and cerium octyl-sulfate precipitates were not found in the literature. Therefore, reaction constants of the cerium sulfate and cerium octyl-sulfate precipitation reactions were calculated using the Gibbs free energy of formation of the precipitates and the corresponding constituent components. All equilibrium calculations were performed using Visual MINTEQ 3.1 software, which is a freeware chemical equilibrium model maintained by Jon Petter Gustafsson at KTH, Sweden. Aqueous and solid species that are not included in the original database of the software were manually added.

Table 1. Reactions involved in the solution equilibrium calculations.

Reaction	lg *K*	Reaction	lg *K*
$2H^+ + C_2O_4^- \rightleftarrows H_2C_2O_4$	5.52	$Fe^{2+} + OH^- \rightleftarrows Fe(OH)^+$	4.60
$H^+ + C_2O_4^{2-} \rightleftarrows HC_2O_4^-$	4.27	$Fe^{2+} + 2OH^- \rightleftarrows Fe(OH)_{2(aq)}$	7.51
$Ce^{3+} + OH^- \rightleftarrows Ce(OH)^{2+}$	5.66	$Fe^{2+} + 3OH^- \rightleftarrows Fe(OH)_3^-$	11.01
$Ce^{3+} + 2OH^- \rightleftarrows Ce(OH)_2^+$	11.70 [a]	$Fe^{2+} + C_2O_4^{2-} \rightleftarrows Fe(C_2O_4)_{(aq)}$	3.97
$Ce^{3+} + 3OH^- \rightleftarrows Ce(OH)_{3(aq)}$	16.00 [a]	$Fe^{2+} + 2C_2O_4^{2-} \rightleftarrows Fe(C_2O_4)_2^{2-}$	5.90
$Ce^{3+} + 4OH^- \rightleftarrows Ce(OH)_4^-$	18.00 [a]	$Fe^{2+} + 2OH^- \rightleftarrows Fe(OH)_{2(c)}$	15.11
$Ce^{3+} + 3OH^- \rightleftarrows Ce(OH)_{3(s)}$	22.11	$Fe^{2+} + 2OH^- \rightleftarrows Fe(OH)_{2(am)}$	14.51
$2Ce^{3+} + 3C_2O_4^{2-} \rightleftarrows Ce_2(C_2O_4)_{3(s)}$	30.18 [b]	$Ca^{2+} + OH^- \rightleftarrows Ca(OH)^+$	1.30
$Ce^{3+} + C_2O_4^{2-} \rightleftarrows Ce(C_2O_4)^+$	6.52 [c]	$Ca^{2+} + C_2O_4^{2-} \rightleftarrows Ca(C_2O_4)_{(aq)}$	3.19
$Ce^{3+} + 2C_2O_4^{2-} \rightleftarrows Ce(C_2O_4)_2^-$	10.48 [c]	$Ca^{2+} + NO_3^- \rightleftarrows Ca(NO_3)^+$	0.5
$Ce^{3+} + 3C_2O_4^{2-} \rightleftarrows Ce(C_2O_4)_3^{3-}$	11.31 [c]	$Ca^{2+} + 2NO_3^- \rightleftarrows Ca(NO_3)_{2(aq)}$	–4.50
$Ce^{3+} + NO_3^- \rightleftarrows Ce(NO_3)^{2+}$	0.81	$Ca^{2+} + C_2O_4^{2-} + H_20 \rightleftarrows Ca(C_2O_4) \cdot H_2O_{(s)}$	8.75
$Ce^{3+} + Cl^- \rightleftarrows CeCl^{2+}$	0.57	$Ca^{2+} + C_2O_4^{2-} + 3H_20 \rightleftarrows Ca(C_2O_4) \cdot 3H_2O_{(s)}$	8.32
$Ce^{3+} + SO_4^{2-} \rightleftarrows Ce(SO_4)^+$	3.64	$Ca^{2+} + 2OH^- \rightleftarrows Ca(OH)_{2(s)}$ Lime	4.70
$Ce^{3+} + 2SO_4^{2-} \rightleftarrows Ce(SO_4)_2^-$	5.1	$Mg^{2+} + OH^- \rightleftarrows Mg(OH)^+$	2.58
$2Ce^{3+} + 3SO_4^{2-} \rightleftarrows Ce_2(SO_4)_{3(s)}$	2.77	$Mg^{2+} + C_2O_4^{2-} \rightleftarrows Mg(C_2O_4)_{(aq)}$	3.62
$2Ce^{3+} + 3SO_4^{2-} + 8H_2O \rightleftarrows Ce_2(SO_4)_3 \cdot 8H_2O_{(s)}$	8.70	$Mg^{2+} + C_2O_4^{2-} \rightleftarrows Mg(C_2O_4)_{(s)}$	5.68
$Al^{3+} + OH^- \rightleftarrows Al(OH)^{2+}$	9.00	$Mg^{2+} + 2OH^- \rightleftarrows Mg(OH)_{2(s)}$ Brucite	10.90
$Al^{3+} + 2OH^- \rightleftarrows Al(OH)_2^+$	17.71	$Mg^{2+} + 2OH^- \rightleftarrows Mg(OH)_{2(s)}$ Active	9.21
$Al^{3+} + 3OH^- \rightleftarrows Al(OH)_{3(aq)}$	25.31	$Mg^{2+} + H_2O - 2H^+ \rightleftarrows MgO_{(s)}$ Periclase	–21.58
$Al^{3+} + 3OH^- \rightleftarrows Al(OH)_{3(s)}$ Gibbsite	34.26	$Nd^{3+} + OH^- \rightleftarrows Nd(OH)^{2+}$	5.82
$Al^{3+} + 4OH^- \rightleftarrows Al(OH)_4^-$	33.00	$Nd^{3+} + 2OH^- \rightleftarrows Nd(OH)_2^+$	10.90 [d]
$2Al^{3+} + 2OH^- \rightleftarrows Al_2(OH)_2^{4+}$	20.31	$Nd^{3+} + 3OH^- \rightleftarrows Nd(OH)_{3(aq)}$	15.60 [d]
$3Al^{3+} + 4OH^- \rightleftarrows Al_3(OH)_4^{5+}$	42.11	$Nd^{3+} + 4OH^- \rightleftarrows Nd(OH)_4^-$	18.61
$Al^{3+} + C_2O_4^{2-} \rightleftarrows Al(C_2O_4)^+$	7.73	$2Nd^{3+} + 2OH^- \rightleftarrows Nd_2(OH)_2^{4+}$	14.11
$Al^{3+} + 2C_2O_4^{2-} \rightleftarrows Al(C_2O_4)_2^-$	13.41	$Nd^{3+} + NO_3^- \rightleftarrows Nd(NO_3)^{2+}$	0.91
$Al^{3+} + 3C_2O_4^{2-} \rightleftarrows Al(C_2O_4)_3^{3-}$	17.09	$Nd^{3+} + C_2O_4^{2-} \rightleftarrows Nd(C_2O_4)^+$	7.21 [c]
$Al^{3+} + HC_2O_4^- \rightleftarrows Al(HC_2O_4)^{2+}$	3.19	$Nd^{3+} + 2C_2O_4^{2-} \rightleftarrows Nd(C_2O_4)_2^-$	11.51 [c]
$Al(OH)^{2+} + C_2O_4^{2-} \rightleftarrows Al(OH)(C_2O_4)$	7.57	$Nd^{3+} + 3C_2O_4^{2-} \rightleftarrows Nd(C_2O_4)_3^{3-}$	14.67 [e]
$Al(OH)_2^+ + C_2O_4^{2-} \rightleftarrows Al(OH)_2(C_2O_4)^-$	7.17	$Nd^{3+} + 3OH^- \rightleftarrows Nd(OH)_{3(s)}$	23.91
$Al(OH)^{2+} + 2C_2O_4^{2-} \rightleftarrows Al(OH)(C_2O_4)_2^{2-}$	11.84	$2Nd^{3+} + 3C_2O_4^{2-} \rightleftarrows Nd_2(C_2O_4)_{3(s)}$	31.11
$Fe^{3+} + OH^- \rightleftarrows Fe(OH)^{2+}$	11.98	$Y^{3+} + OH^- \rightleftarrows Y(OH)^{2+}$	6.20
$Fe^{3+} + 2OH^- \rightleftarrows Fe(OH)_2^+$	22.25	$Y^{3+} + 2OH^- \rightleftarrows Y(OH)_2^+$	11.60 [f]
$Fe^{3+} + 3OH^- \rightleftarrows Fe(OH)_{3(aq)}$	27.00	$Y^{3+} + 3OH^- \rightleftarrows Y(OH)_{3(aq)}$	16.00 [f]
$Fe^{3+} + 4OH^- \rightleftarrows Fe(OH)_4^-$	33.30	$Y^{3+} + 4OH^- \rightleftarrows Y(OH)_4^-$	19.50 [f]
$2Fe^{3+} + 2OH^- \rightleftarrows Fe_2(OH)_2^{4+}$	25.11	$2Y^{3+} + 2OH^- \rightleftarrows Y_2(OH)_2^{4+}$	13.81
$3Fe^{3+} + 4OH^- \rightleftarrows Fe_3(OH)_4^{5+}$	49.71	$Y^{3+} + NO_3^- \rightleftarrows Y(NO_3)^{2+}$	0.40
$Fe^{3+} + C_2O_4^{2-} \rightleftarrows Fe(C_2O_4)^+$	9.15	$Y^{3+} + C_2O_4^{2-} \rightleftarrows Y(C_2O_4)^+$	6.74
$Fe^{3+} + 2C_2O_4^{2-} \rightleftarrows Fe(C_2O_4)_2^-$	15.45	$Y^{3+} + 2C_2O_4^{2-} \rightleftarrows Y(C_2O_4)_2^-$	10.10 [g]
$Fe^{3+} + 3C_2O_4^{2-} \rightleftarrows Fe(C_2O_4)_3^{3-}$	19.83	$Y^{3+} + 3C_2O_4^{2-} \rightleftarrows Y(C_2O_4)_3^{3-}$	11.47 [g]
$2Fe^{3+} + 3H_2O - 6H^+ \rightleftarrows Fe_2O_{3(s)}$ Hematite	1.42	$Y^{3+} + 3OH^- \rightleftarrows Y(OH)_{3(s)}$	24.51
		$2Y^{3+} + 3C_2O_4^{2-} \rightleftarrows Y_2(C_2O_4)_{3(s)}$	28.27 [g]

Note: a [24], b [25], c [26], d [27], e [28], f [29], and g [30]; the other reaction constants except $Ce_2(SO_4)_{3(s)}$ and $Ce_2(SO_4)_3 \cdot 8H_2O_{(s)}$ formations were referred to the database of Visual MINTEQ 3.1 software; the reaction constants for $Ce_2(SO_4)_{3(s)}$ and $Ce_2(SO_4)_3 \cdot 8H_2O_{(s)}$ formations were calculated using the Gibbs free energy of formation of Ce^{3+} (–161.809 kcal/mol, database of HSC Chemistry 6 software), SO_4^{2-} (–177.907 kcal/mol [31]), H_2O (–56.678 kcal/mol [31]), $Ce_2(SO_4)_{3(s)}$ (–861.115 kcal/mol [31]), and $Ce_2(SO_4)_3 \cdot 8H_2O_{(s)}$ (–1322.620 kcal/mol [31]).

3. Results and discussion

3.1 Precipitation characteristics of Ce^{3+} in the absence of contaminant metal ions

As one of the most geologically abundant rare earth elements, the precipitation recovery of 1×10^{-4} mol/L Ce^{3+} from solutions in the absence of other metal ions (e.g., Al^{3+}, Fe^{3+}, Mg^{2+}, Ca^{2+}, and Fe^{2+}) was first determined. The selection of the cerium concentration being 1×10^{-4} mol/L, which was used as an input in the calculations, is based on prior studies of rare earth recovery from acid coal mine leachates [21,32]. As shown in Fig. 1(a), both solution acidity and oxalate concentration largely affect the recovery of cerium. For all the oxalate concentrations investigated in this study, at low pH values, cerium recovery sharply increases with increased pH, which is attributable to the improvement in the dissociation of oxalic acid molecules. After reaching a critical pH value, the recovery stabilizes to a fixed value and barely changes with further increases in pH. For example, when an oxalate concentration of 1×10^{-4} mol/L is employed, a recovery value of 56% is obtained by elevating pH from 1.5 to 2.5; whereas a further increase in pH to 5.0 only provides an additional 5.5% gain in the recovery. This result is likely due to the insufficient oxalate in the system. As indicated by the stoichiometric ratio of cerium to oxalate in the precipitation reaction (see Table 1), a precipitant dosage of greater than1.5×10^{-4} mol/L is required to achieve satisfactory recovery.

Using higher concentrations of oxalate, changes in the recovery as a function of pH show a similar pattern as the system containing 1×10^{-4} mol/L oxalate, but larger recovery values are achieved. As shown in Fig. 1(a), 95% of cerium is precipitated at pH 2.5 with 2×10^{-4} mol/L oxalate, and the recovery is increased to nearly 100% by elevating pH to 5.0. Rather than insufficient precipitant, the slight gains in recovery in the pH range of 2.5–5.0 are due to the depletion of cerium ions, resulting from the extensive precipitation reactions occurring at lower pH. Cerium concentration of 1 mg/L (7.14×10^{-6} mol/L) in residual solutions after selective precipitation have been used as an acceptable target level [19], which corresponds to approximately 93% recovery when 1×10^{-4} mol/L of cerium occurs. As shown, in order to achieve the acceptable recovery, a minimum pH of around 2.3 is required when using 2×10^{-4} mol/L oxalate. Lower pH values of around 2.0 and 1.8 can be used for higher oxalate doses of 3×10^{-4} and 4×10^{-4} mol/L, respectively. In addition to the reduced cost of pH adjustment, another potential benefit of conducting oxalic acid precipitation under more acidic conditions is that higher-grade products can be obtained since the oxalate precipitates of contaminant metal ions barely form (see following sections).

In the extraction process of rare earths from solid resources, minerals acids, including sulfuric, nitric, and hydrochloric acids, are frequently applied as lixiviants. Therefore, anionic species, such as NO_3^-, Cl^-, and SO_4^{2-}, normally occur in the REE-concentrated solutions that are processed using oxalic acid precipitation. The effects of the anions on the recovery of cerium were also evaluated through solution equilibrium calculations. As shown in Fig. 1(b-d), the precipitation efficiency of cerium is impaired in the presence of NO_3^-, Cl^-, or SO_4^{2-}. For example,

cerium recovery at pH 2.0 is decreased from 96% to 79% and 77%, respectively, in the presence of 0.5 mol/L NO_3^- and Cl^-. Moreover, cerium oxalate precipitate does not form at pH 2.0 when 0.1 mol/L SO_4^{2-} occurs in the system. Therefore, NO_3^- and Cl^- are more favorable than SO_4^{2-} in the rare earth oxalic acid precipitation process. It is worth noting that rare earths have been recovered and purified through sulfate, double sulfate, and octyl-sulfate precipitations [19,20,31]. However, solution equilibrium calculation results showed that these precipitates do not occur in the current systems. The negative impacts caused by the anions primarily result from their capabilities to form complexes with rare earths (e.g., $CeCl^{2+}$, $Ce(NO_3)^{2+}$, and $Ce(SO_4)^+$). As indicated by the larger stability constant of $Ce(SO_4)^+$ relative to the other two species ($10^{3.64}$ versus $10^{0.57}$ and $10^{0.81}$), sulfate has a stronger complexing ability towards Ce^{3+}, which explains the reduced precipitation efficiency.

Fig. 1. Precipitation behavior of Ce^{3+} from solutions containing 1×10^{-4} mol/L Ce^{3+} in the absence of other metal ions as a function of pH. (a) Oxalate dosage effect in the absence of NO_3^-, Cl^-, and SO_4^{2-}; (b) NO_3^-, (c) Cl^-, and (d) SO_4^{2-} effects when using 4×10^{-4} mol/L oxalate. (Black dashed line presents the target recovery of 93%)

3.2 Precipitation characteristics of Ce^{3+} in the presence of contaminant metal ions

Contaminant metal ions, such as Al^{3+}, Fe^{3+}, Mg^{2+}, Ca^{2+}, and Fe^{2+}, are normally introduced into REE-concentrated solutions due to low extraction selectivity in recovery processes prior to oxalic acid precipitation. Significant impacts on the precipitation efficiency of REEs may be caused by these metal ions. To rigorously assess this impact, solution equilibrium calculations were conducted by considering the reactions listed in Table 1.

3.2.1 Effect of Al^{3+} on precipitation characteristics of Ce^{3+}

As mentioned above, 56% and 95% of Ce^{3+} can be recovered at pH 2.5 using 1×10^{-4} mol/L and 2×10^{-4} mol/L oxalic acid, respectively, from a solution containing 1×10^{-4} mol/L Ce^{3+} (see Fig. 1(a)). This behavior changes drastically, though, with the addition of Al^{3+} into the solution. As shown in Fig. 2(a), when 1×10^{-4} mol/L Al^{3+} and 1×10^{-4} mol/L oxalate occur in a solution, cerium starts to precipitate at around pH 2.0, which is higher than the pH observed in the system in the absence of Al^{3+} (pH 1.5, see Fig. 1(a)). Furthermore, changes in cerium recovery as a function of pH in the absence and presence of Al^{3+} are different. As shown, cerium recovery is only increased to 8% by elevating pH to 2.5, and the recovery remains nearly unchanged until the pH is increased to around 4.1, after which considerable improvements in the recovery occur. The mechanisms that cause this behavior are apparent when investigating the speciation of Al^{3+}. The reactions listed in Table 1 show that Al^{3+} forms a number of complexes with oxalate in solution, such as $Al(C_2O_4)^+$, $Al(C_2O_4)_2^-$, and $Al(HC_2O_4)^{2+}$. The complexing reactions will reduce the concentration of oxalate available for precipitating cerium. Therefore, the recovery of REE at pH values less than 4.1 is largely reduced in the presence of Al^{3+}. However, gibbsite ($Al(OH)_{3(s)}$)

forms in the solution at pH 4.1, leading to the elimination of Al^{3+}, thereby the concentration of free oxalate species is increased. This reaction contributes to the increases in cerium recovery in the pH range of 4.1–5.0. A similar pattern is observed when oxalate concentration is elevated to 2×10^{-4} mol/L; whereas higher recovery values are obtained, which is primarily due to that more oxalate species are available for precipitating cerium. As indicated by the rapid increase in the recovery starting from pH 4.1, gibbsite also forms in the system, which likely cause a reduction in the purity of final product. Therefore, in order to recover 93% of the cerium without sacrificing product purity, oxalate dosages of 3×10^{-4} mol/L or higher are required.

A solution containing much more Al^{3+} compared with Ce^{3+} (1×10^{-3} mol/L versus 1×10^{-4} mol/L) was also investigated. As shown in Fig. 2(b), cerium precipitation does not occur until pH is elevated to around 3.8, however nearly 100% of the cerium is precipitated by further elevating pH to around 4.5. This phenomenon indicates that at pH below 3.8, oxalate species are primarily complexed with Al^{3+}, thereby Ce^{3+} stays in the solution as aqueous species. However, the majority of the Al^{3+} is precipitated in the form of gibbsite at pH 3.8, which increases the amount of free oxalate species in the solution. Therefore, cerium precipitation occurs when the pH exceeds 3.8. In order to achieve 93% recovery of cerium prior to gibbsite formation, oxalate dosages of greater than 1.4×10^{-3} mol/L are required. The impact of Al^{3+} on cerium precipitation can be better explained by plotting cerium recovery against Al^{3+} concentration. As shown in Fig. 2(c), in a solution containing 1×10^{-4} mol/L Ce^{3+} and 4×10^{-4} mol/L oxalate, the precipitation recovery of cerium considerably decreases as Al^{3+} concentration elevates.

The dosage of oxalate required for recovering 93% of cerium at pH 1.5 and 2.0 in the presence and absence of NO_3^- were calculated for solutions containing 1×10^{-4} mol/L Ce^{3+} and varying concentrations of Al^{3+}. As shown in Fig. 2(d), for both systems, the oxalate dosage increases linearly with elevations in Al^{3+} concentration. As indicated by the slope of the plots, for each unit increase in Al^{3+} concentration (e.g., 1×10^{-4} mol/L), oxalate dosage needs to be increased by approximately 1.2 units (e.g., 1.2×10^{-4} mol/L) to achieve the target recovery. Moreover, this Fig. also shows the deleterious impact of NO_3^- in solutions containing Al^{3+}. For a fixed pH and Al^{3+} concentration, more oxalate is needed to reach the target recovery in solutions containing NO_3^-. In addition, the slopes of lines are increased due to the appearance of NO_3^- (e.g., 1.34 for 0.5 mol/L NO_3^-). Therefore, the negative impacts of Al^{3+} on the oxalic acid precipitation recovery of cerium are amplified by NO_3^-, which can be explained by the complexation between NO_3^- and Ce^{3+}.

Fig. 2. Effects of Al^{3+} on the precipitation recovery of Ce^{3+} from solutions containing 1×10^{-4} mol/L Ce^{3+}: (a) Cerium recovery as a function of pH in the presence of 1×10^{-4} mol/L Al^{3+}; (b) Cerium recovery as a function of pH in the presence of 1×10^{-3} mol/L Al^{3+}; (c) Cerium recovery as a function of Al^{3+} concentration using 4×10^{-4} mol/L oxalate; (d) Oxalate dosages required to

achieve 93% recovery in the presence and absence of NO_3^- as a function of Al^{3+} concentration. (Black dashed line presents the target recovery of 93%)

3.2.2 Effect of Fe^{3+} on precipitation characteristics of Ce^{3+}

The effects of Fe^{3+} on the oxalate precipitation characteristics of Ce^{3+} were also investigated using the same approach as that of Al^{3+}. As shown in Fig. 3(a), when using 1×10^{-4} mol/L oxalate to recover cerium from a solution containing 1×10^{-4} mol/L Ce^{3+} and 1×10^{-4} mol/L Fe^{3+}, the precipitation reaction starts at around pH 1.9, which is higher than the pH observed in the absence of Fe^{3+} (pH 1.5, see Fig. 1(a)). This contrast is primarily due to complexation reactions between Fe^{3+} and oxalate. In addition, as shown in Fig. 3(b), precipitation of Fe^{3+} occurs starting from around pH 1.6, and the recovery increases to 40% at pH 1.9. Based on the reactions involved in the solution equilibrium calculations (Table 1), it can be concluded that ferric ions in the solution are precipitated in the form of hematite. The partial removal of ferric ions from the solution in the pH range of 1.6–1.9 promotes the occurrence of cerium oxalate precipitation at pH 1.9, since a portion of oxalate originally complexed with ferric ions is released and available for precipitating cerium. As shown, iron recovery increases more rapidly after pH 1.9, which can be explained by the decrease in the concentration of oxalate species due to cerium oxalate precipitation, leading to more free ferric species that likely form hematite. Therefore, Ce^{3+} and Fe^{3+} are precipitated simultaneously in the solution at pH larger than 1.9. Comparisons between Fig. 3(a, b) indicate that cerium oxalate precipitation occurs prior to hematite formation when using higher oxalate dosages (2×10^{-4} mol/L and 3×10^{-4} mol/L). However, for both dosage levels, the acceptable recovery of cerium (93%) cannot be obtained by elevating pH without hematite formation. Rapid increases in recovery at pH 1.9 and pH 2.0 are observed from the plots of 2×10^{-4} mol/L and 3×10^{-4} mol/L oxalate, respectively, which corroborates this conclusion. In order to obtain a high-purity cerium product at the target recovery, oxalate dosage should be greater than 4×10^{-4} mol/L.

The cerium recovery as a function of ferric ion concentration is shown in Fig. 3(c). As shown, at pH 1.5, the presence of around 2.5×10^{-4} mol/L Fe^{3+} reduces the recovery from 76% to 0%; whereas at higher pH, the recovery is first decreased and then remains constant. As mentioned above, this phenomenon can be explained by the collectively function of ferric-oxalate complexation and ferric ion precipitation. As shown in Fig. 3(d), the oxalate dosage required to achieve the target recovery at pH 2 linearly increases from around 3×10^{-4} to 1×10^{-3} mol/L when Fe^{3+} concentration elevates from 0 mol/L to 4×10^{-4} mol/L. After that, the required dosage remains unchanged due to the formation of hematite. Since ferric ions are not precipitated at pH 1.5, the required dosage continuously increases over the investigated Fe^{3+} concentration range (0 mol/L to 1×10^{-3} mol/L). As indicated by the slope of the plot at pH 1.5, for each unit increase in Fe^{3+} concentration (e.g., 1×10^{-4} mol/L), oxalate dosage needs to be increased by approximately 1.68 units (e.g., 1.68×10^{-4} mol/L) to achieve the target recovery. Therefore, Fe^{3+} imposes a more

significant impact on the oxalate precipitation of cerium compared with Al^{3+}. Moreover, the plot of 0.1 mol/L NO_3^- at pH 2.0 has a larger slope of 1.86, thereby the negative impacts of Fe^{3+} on the oxalic acid precipitation of cerium are amplified by NO_3^-.

Fig. 3. Effects of Fe^{3+} on precipitation recovery of Ce^{3+} from solutions containing 1×10^{-4} mol/L Ce^{3+}. (a) Cerium recovery as a function of pH in the presence of 1×10^{-4} mol/L Fe^{3+}; (b) Iron recovery as a function of pH in the cerium precipitation process; (c) Cerium recovery as a function of Fe^{3+} concentration using 4×10^{-4} mol/L oxalate; (d) Oxalate dosages required to achieve 93% recovery in the presence and absence of NO_3^- as a function of Fe^{3+} concentration. (Black dashed line presents the target recovery of 93%)

3.2.3 Effects of Fe^{2+}, Mg^{2+}, and Ca^{2+} on precipitation characteristics of Ce^{3+}

In addition to the selected trivalent metal cations, the effects of several divalent metal ions that are most commonly found in REE-concentrated solutions were also studied through solution equilibrium calculations. As shown in Fig. 4(a-c), cerium recovery slightly decreases with increases in Fe^{2+}, Mg^{2+}, and Ca^{2+} concentration, thereby it can be concluded that the divalent metal ions have negligible impacts over the investigated concentration range (0 to 1×10^{-3} mol/L). In addition, since hydroxide/oxide precipitates of the cations do not occur under the acidic conditions, the purity of cerium oxalate product will not be affected. However, as indicated by the reactions listed in Table 1, oxalate precipitates of Mg^{2+} and Ca^{2+} are likely formed in the presence of oxalate, which need to be considered in real practice. In the current systems (pH 1.5–2.5, 1×10^{-4} mol/L Ce^{3+}, 4×10^{-4} mol/L oxalate, and 0 – 1×10^{-3} mol/L divalent metal ions), magnesium oxalate is not formed, whereas the oxalate precipitate of calcium occurs at pH 2.5 when calcium concentration exceeds 6×10^{-4} mol/L (Fig. 4(d)). In this case, the purity of the precipitation product will be impaired.

The dosages of oxalate required to achieve 93% cerium recovery were calculated. As shown in Fig. 5, the impacts of the divalent metal ions on the required dosages are negligible. Based on the slopes of the plots, it can be told that oxalate dosage needs to increase by 1.1×10^{-6} – 1.5×10^{-6} mol/L for each 1×10^{-4} mol/L increase in the divalent metal ion concentration.

Fig. 4. Precipitation recovery of Ce^{3+} from solutions containing 1×10^{-4} mol/L Ce^{3+}, 4×10^{-4} mol/L oxalate, and different concentrations of Fe^{2+} (a), Mg^{2+} (b), and Ca^{2+} (c), as well as species distribution of Ca^{2+} at pH 2.50 (d) as a function of Ca^{2+} concentration.

Fig. 5. Oxalate dosages required to achieve 93% recovery of Ce^{3+} as a function of Fe^{2+}, Mg^{2+}, and Ca^{2+} concentrations (Ce^{3+} concentration equals 1×10^{-4} mol/L; pH equals 2.0).

3.3 Precipitation characteristics of Nd^{3+} and Y^{3+} in the presence of contaminant metal ions

The discussions above indicate that contaminant metal ions including Al^{3+} and Fe^{3+} have considerable impacts on the reagent consumption and precipitation recovery of Ce^{3+} when using oxalic acid as a precipitant. To obtain a more comprehensive understanding of this topic, solution equilibrium calculations were also performed on solutions containing other REEs (Nd^{3+} and Y^{3+}). As shown in Fig. 6(a), the recovery of Nd^{3+} and Y^{3+} as a function of pH shows a similar pattern as Ce^{3+}, namely rapid increases in the recovery occur at low pH, and the recovery maintains nearly unchanged at high pH. In addition, it can be observed that precipitation efficiencies of the three REEs follow the order of $Nd^{3+} > Ce^{3+} > Y^{3+}$. This finding corroborates a conclusion reported in prior studies that REEs in the middle of the lanthanide series in the periodic table of elements are more likely precipitated compared with other REEs when using oxalate as a precipitant [32,33]. Moreover, as shown in Fig. 6(b), when NO_3^- occurs in solution, the recovery of Nd^{3+} and Y^{3+} is decreased, which is the same as the phenomenon observed for Ce^{3+} and can be explained by the formation of rare earth-nitrite complexes.

The effects of Al^{3+}, Fe^{3+}, Fe^{2+}, Ca^{2+}, and Mg^{2+} on oxalate dosages required to achieve an acceptable level of recovery of Nd^{3+} and Y^{3+} from solutions containing 1×10^{-4} mol/L of the REEs are shown in Fig. 7. The target recovery was fixed at 93% for comparison with Ce^{3+}. As shown, the divalent metal ions, including Fe^{2+}, Ca^{2+}, and Mg^{2+}, show minor impacts on the precipitation recovery of Nd^{3+} and Y^{3+}; whereas the required dosages considerably increase when Al^{3+} and Fe^{3+} occur in the solutions. In addition, due to the formation of hematite, when Fe^{3+} concentration exceeds 5×10^{-4} mol/L, required dosages for the Nd^{3+} precipitation maintain unchanged. This phenomenon agrees with the findings from the solution equilibrium calculations of Ce^{3+} (see Fig. 3(d)). Based on the slope of the Fe^{3+} plot in the range of 0 mol/L to 5×10^{-4} mol/L (Fig. 7(a)), it can be concluded that for each unit increase in Fe^{3+} concentration (e.g., 1×10^{-4} mol/L), the required oxalate dosage for recovering 93% of Nd^{3+} shall increase by 1.6 units (e.g., 1.6×10^{-4} mol/L). However, in the concentration range of 0 mol/L to 1×10^{-3} mol/L, only 1.2 units increase in oxalate dosage are required for a unit increase in Al^{3+} concentration. Moreover, as shown in Fig. 7(b), Al^{3+} and Fe^{3+} impose more significant impacts on Y^{3+} precipitation compared with Nd^{3+}. For example, based on the slope of the Fe^{3+} plot, 3.5×10^{-4} mol/L increase in oxalate concentration is required when Fe^{3+} concentration in the solution is increased by 1×10^{-4} mol/L. This contrast is due to the larger solubility product of $Y_2(C_2O_4)_{3(s)}$ than $Ce_2(C_2O_4)_{3(s)}$ and $Nd_2(C_2O_4)_{3(s)}$ oxalates ($10^{-28.27}$ versus $10^{-30.18}$ and $10^{-31.11}$, see Table 1). In addition, resulting from the same reason, nearly an order of magnitude higher dosage of oxalate is required for achieving the same recovery of Y^{3+}as Nd^{3+} and Ce^{3+}.

Fig. 6. Effects of pH (a) and NO_3^- (b) on the precipitation characteristics of Nd^{3+} and Y^{3+} from solutions containing 1×10^{-4} mol/L rare earth and 4×10^{-4} mol/L oxalate. (Black dashed line presents the target recovery of 93%).

Fig. 7. Oxalate dosages required to achieve 93% recovery of Nd^{3+} (a) and Y^{3+} (b) as a function of Al^{3+}, Fe^{3+}, Fe^{2+}, Ca^{2+}, and Mg^{2+} concentrations (rare earth concentration equals 1×10^{-4} mol/L; pH equals 2.0).

4. Conclusions

In this study, the effects of contaminant metal ions that frequently occur in REE-enriched solutions on the precipitation recovery of REEs using oxalic acid as a precipitant were investigated through solution equilibrium calculations. Based on the calculations performed on solutions containing 1×10^{-4} mol/L of selected REEs (Ce^{3+}, Nd^{3+}, and Y^{3+}), it was found that Al^{3+} and Fe^{3+} have greater impacts on the precipitation efficiency compared with divalent metal ions (Fe^{2+}, Mg^{2+}, and Ca^{2+}). For example, when Al^{3+} and Fe^{3+} concentrations in the solutions are increased by 1×10^{-4} mol/L, oxalate dosage needs to be increased by 1.2×10^{-4} and 1.68×10^{-4} mol/L, respectively, in order to achieve the target cerium recovery level of 93%. However, less than 1.5×10^{-6} mol/L increase in oxalate dosage is required in the presence of the divalent metal ions. In addition, based on the recovery values of Ce^{3+}, Nd^{3+}, and Y^{3+} calculated as a function of pH, it was concluded that precipitation efficiencies of the three REEs using oxalic acid as the precipitant follow the order of $Nd^{3+} > Ce^{3+} > Y^{3+}$. This finding corroborates a conclusion from prior studies that REEs in the middle of the lanthanide series in the periodic table of elements are more likely precipitated using oxalate compared with other REEs.

In addition to the impacts on oxalate dosages required to achieve the acceptable recovery, the presence of the contaminant metal ions also reduce the purity of rare earth oxalate product. For example, solution chemistry calculation results of this study show that Fe^{3+} and Ca^{2+} are likely precipitated in the form of hematite and $Ca(C_2O_4)\cdot H_2O_{(s)}$, respectively, together with REEs under certain conditions. The occurrence of the undesirable precipitates can be avoided by conducting rare earth oxalate precipitation under low pH conditions. Moreover, anionic species, especially SO_4^{2-}, were also found to considerably reduce the precipitation efficiency, primarily due to their complexing abilities with the REEs.

References

1. Wu SX, Wang LS, Zhao LS, Zhang P, Hassan ES, Moudgil B, et al. Recovery of rare earth elements from phosphate rock by hydrometallurgical processes – A critical review. *Chem Eng J*. 2018;335:774.

2. Binnemans K, Jones PT, Blanpain B, Gerven TV, Yang YX, Walton A, et al. Recycling of rare earths: A critical review. *J Clean Prod*. 2013;51:1.

3. Zhang WC, Noble A. Mineralogy characterization and recovery of rare earth elements from the roof and floor materials of the Guxu coalfield. *Fuel*. 2020;270:117533.

4. Jyothi RK, Thenepalli T, Ahn JW, Parhi PK. Graphical abstract Review of rare earth element recovery from secondary resources for clean energy. *J Clean Prod*. 2020:122048.

5. Omodara L, Pitkäaho S, Turpeinen EM, Saavalainen P, Oravisjärvi K, Keiski RL. Recycling and substitution of light rare earth elements, cerium, lanthanum, neodymium, and praseodymium from end-of-life applications - A review. *J Clean Prod*. 2019;236:117573.

6. Zhang WC, Rezaee M, Bhagavatula A, Li YG, Groppo J, Honaker R. A review of the occurrence and promising recovery methods of rare earth elements from coal and coal by-products. *Int J Coal Prep Util*. 2015;35(6):281.

7. Talan D, Huang QQ. Separation of thorium, uranium, and rare earths from a strip solution generated from coarse coal refuse. *Hydrometallurgy*. 2020;197:105446.

8. Yang XB, Werner J, Honaker RQ. Leaching of rare Earth elements from an Illinois basin coal source. *J Rare Earths*. 2019;37(3):312.

9. Behera SS, Panda SK, Mandal D, Parhi PK. Ultrasound and Microwave assisted leaching of neodymium from waste magnet using organic solvent. *Hydrometallurgy*. 2019;185:61.

10. Behera SS, Parhi PK. Leaching kinetics study of neodymium from the scrap magnet using acetic acid. *Sep Purif Technol*. 2016;160:59.

11. Liu ZY, Wu JM, Liu XY, Wang W, Li ZW, Xu RJ, et al. Recovery of neodymium, dysprosium, and cobalt from NdFeB magnet leachate using an unsymmetrical dialkylphosphinic acid extractant, INET-3. *J Rare Earths*. 2020;38(10):1114.

12. Nie DP, Xue A, Zhu MY, Zhang Y, Cao JJ. Separation and recovery of associated rare earths from the Zhijin phosphorite using hydrochloric acid. *J Rare Earths*. 2019;37(4):443.

13. Jordens A, Cheng YP, Waters KE. A review of the beneficiation of rare earth element bearing minerals. *Miner Eng*. 2013;41:97.

14. Sadri F, Nazari AM, Ghahreman A. A review on the cracking, baking and leaching processes of rare earth element concentrates. *J Rare Earths*. 2017;35(8):739.

15. Jha MK, Gupta D, Lee JC, Kumar V, Jeong J. Solvent extraction of platinum using amine based extractants in different solutions: A review. *Hydrometallurgy*. 2014;142:60.

16. Demol J, Ho E, Soldenhoff K, Senanayake G. The sulfuric acid bake and leach route for processing of rare earth ores and concentrates: A review. *Hydrometallurgy*. 2019;188:123.

17. Abhilash SS, Meshram P, Pandey BD. Metallurgical processes for the recovery and recycling of lanthanum from various resources - A review. *Hydrometallurgy*. 2016;160:47.

18. Chi RA, Xu ZH. A Solution Chemistry Approach to the Study of Rare Earth Element

Precipitation by Oxalic Acid. *Metall Mater Trans B Process Metall Mater Process Sci*. 1999;30:189.

19. Han KN. Characteristics of precipitation of rare earth elements with various precipitants. *Minerals*. 2020;10(2). doi:10.3390/min10020178

20. Kul M, Topkaya Y, Karakaya İ. Rare earth double sulfates from pre-concentrated bastnasite. 2008;93:129.

21. Zhang WC, Honaker R. Process development for the recovery of rare earth elements and critical metals from an acid mine drainage. *Miner Eng*. 2020;153:106382.

22. Jorjani E, Shahbazi M. The production of rare earth elements group via tributyl phosphate extraction and precipitation stripping using oxalic acid. *Arab J Chem*. 2016;9:S1532.

23. Josso P, Roberts S, Teagle DAH, Pourret O, Herrington R, Ponce de Leon Albarran C. Extraction and separation of rare earth elements from hydrothermal metalliferous sediments. *Miner Eng*. 2018;118:106.

24. Zhang WC, Honaker R. Surface charge of rare earth phosphate (monazite) in aqueous solutions. *Powder Technol*. 2017;318:263.

25. Xiong YL. Organic species of lanthanum in natural environments: Implications to mobility of rare earth elements in low temperature environments. *Appl Geochemistry*. 2011;26(7):1130.

26. Crouthamel CE, Martin DS, Crouthamel CE. Solubility of the Rare Earth Oxalates and Complex Ion Formation in Oxalate Solution. II. Neodymium and Cerium(III). *J Am Chem Soc*. 1951;73(2):569.

27. Poitrasson F, Oelkers E, Schott J, Montel JM. Experimental determination of synthetic NdPO4 monazite end-member solubility in water from 21°C to 300°C: Implications for rare earth element mobility in crustal fluids. *Geochim Cosmochim Acta*. 2004;68(10):2207.

28. Rodríguez-Ruiz I, Teychené S, Vitry Y, Biscans B, Charton S. Thermodynamic modeling of neodymium and cerium oxalates reactive precipitation in concentrated nitric acid media. *Chem Eng Sci*. 2018;183:20.

29. Baes CF, Mesmer RE. The Hydrolysis of Cations 1976. *Malabar, Fla RE Krieger*.

30. Feibush AM, Rowley K, Gordon L. Solubility of Yttrium Oxalate. *Anal Chem*. 1958;30(10):1610.

31. Kim E, Osseo-Asare K. Aqueous stability of thorium and rare earth metals in monazite hydrometallurgy: Eh-pH diagrams for the systems Th-, Ce-, La-, Nd- (PO 4)-(SO 4)-H 2O at 25 °c. *Hydrometallurgy*. 2012;113-114:67.

32. Zhang WC, Honaker RQ. Rare earth elements recovery using staged precipitation from a leachate generated from coarse coal refuse. *Int J Coal Geol*. 2018;195:189.

33. Chung DY, Kim EH, Lee EH, Yoo JH. Solubility of rare earth oxalate in oxalic and nitric acid media. *J Ind Eng Chem*. 1998;4(4):277.

Graphical abstract:

During the selective precipitation process of rare earths using oxalic acid, consumption of the precipitant is largely increased by trivalent metal ions, such as Al^{3+} and Fe^{3+}, while divalent metal ions impose minor impact.

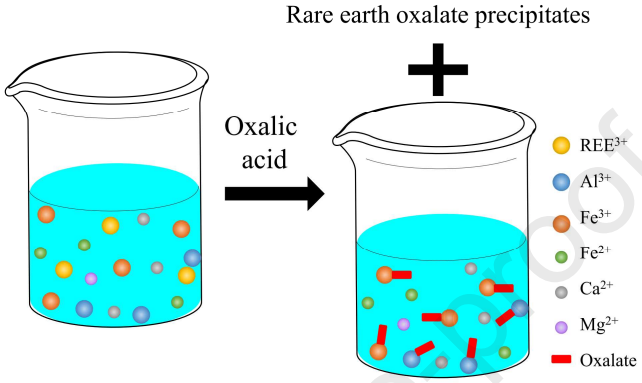

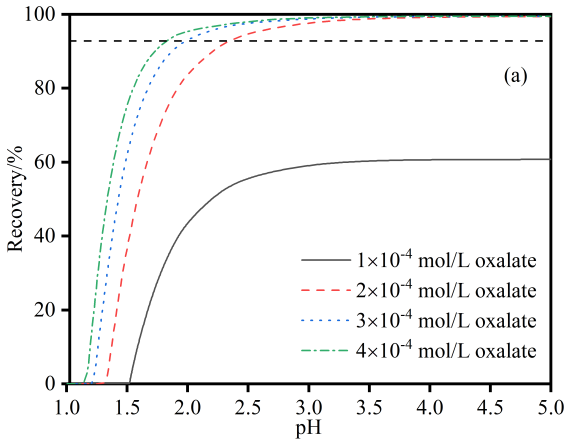

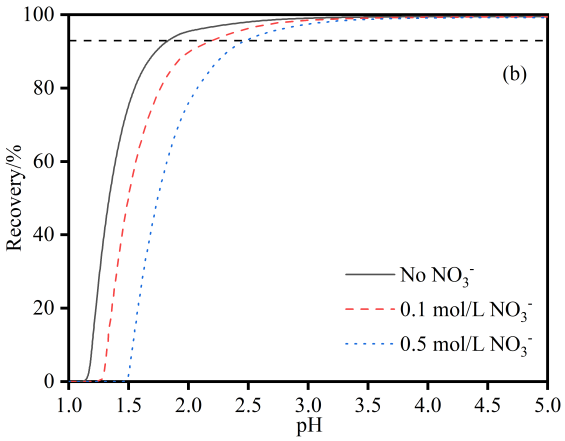

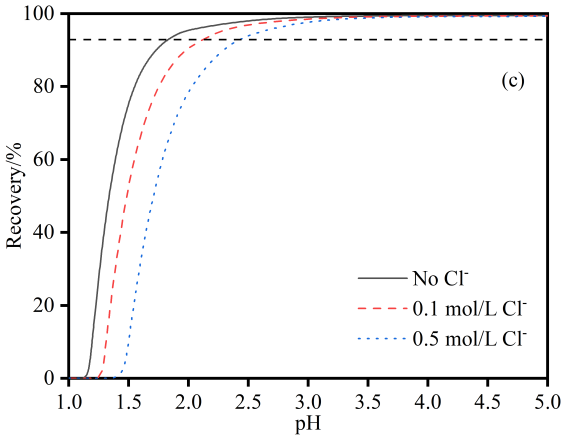

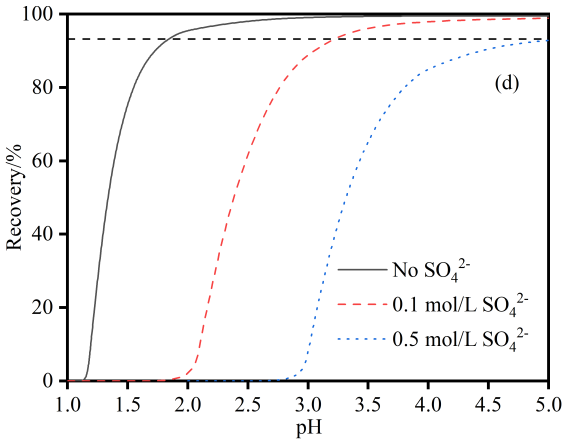

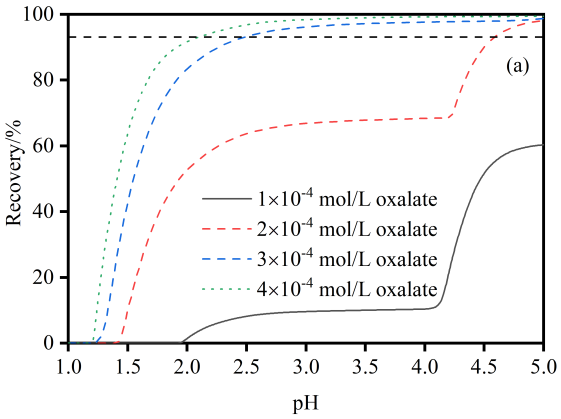

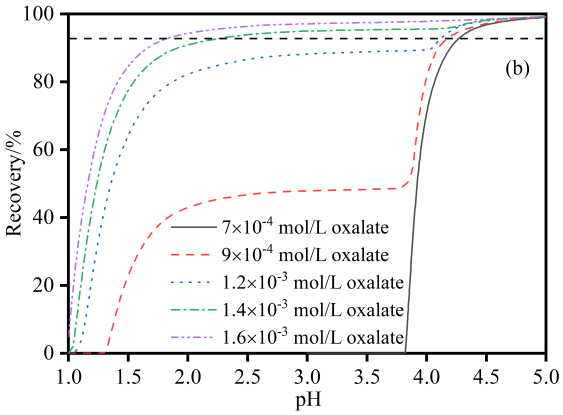

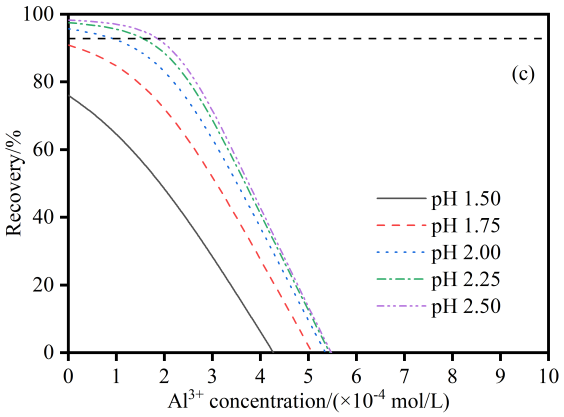

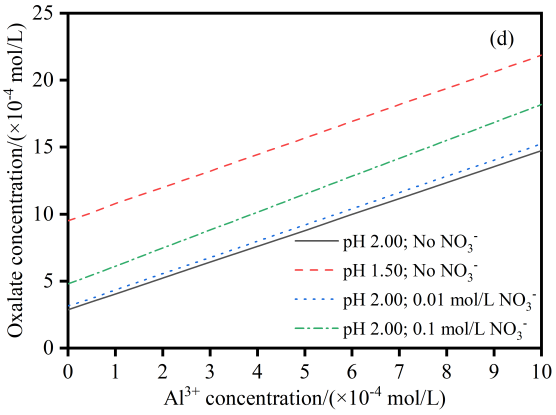

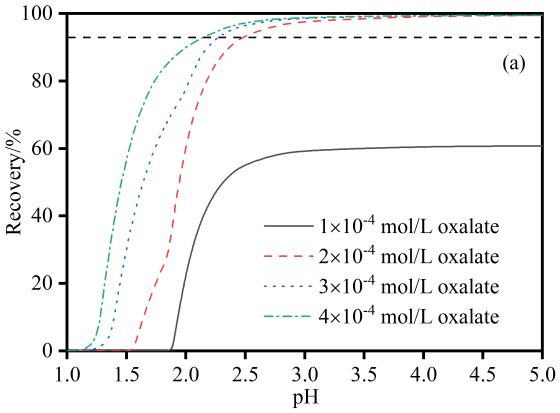

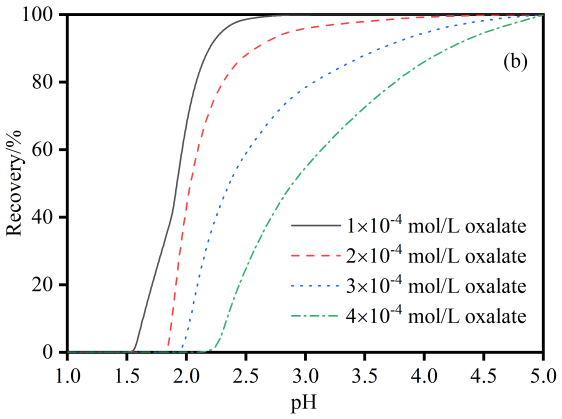

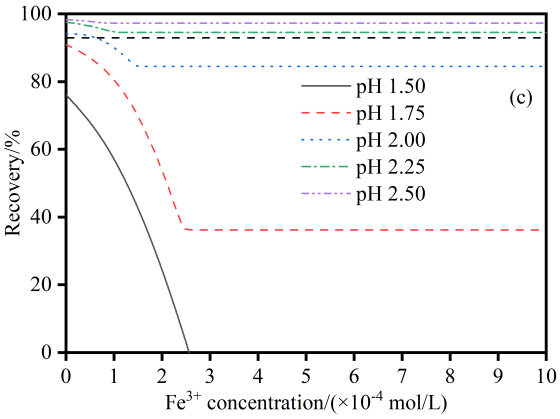

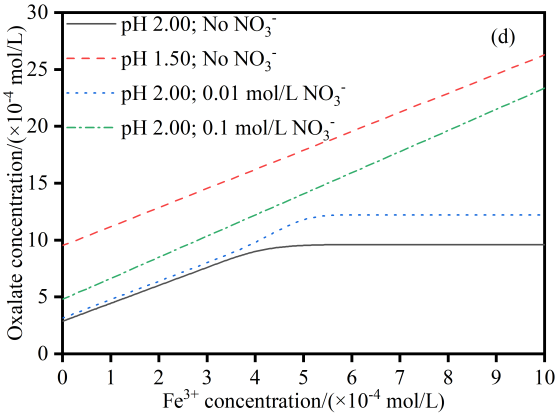

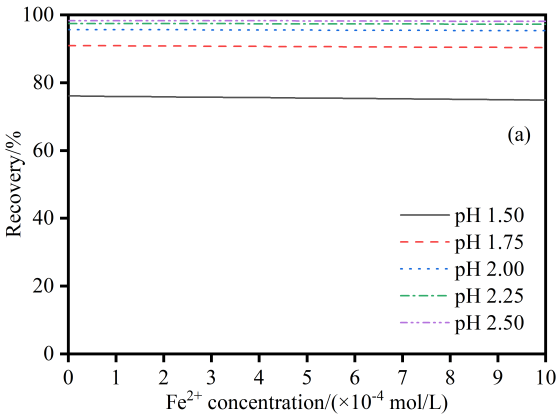

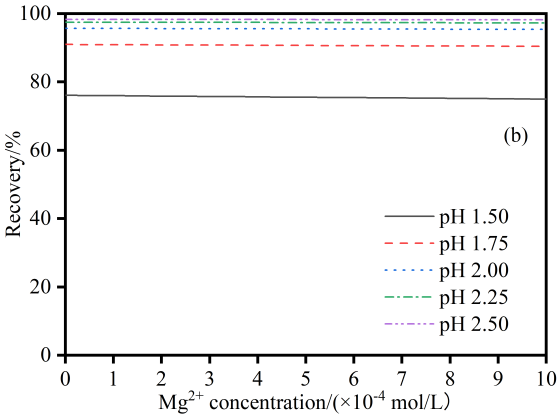

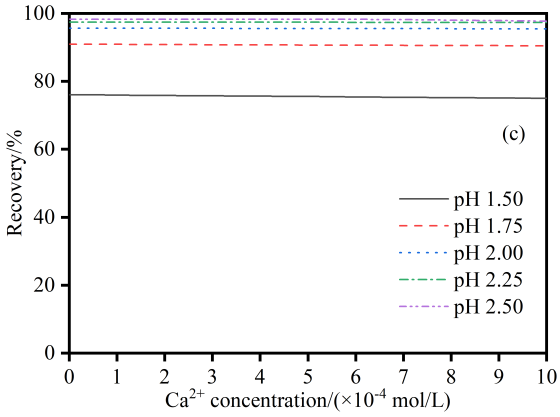

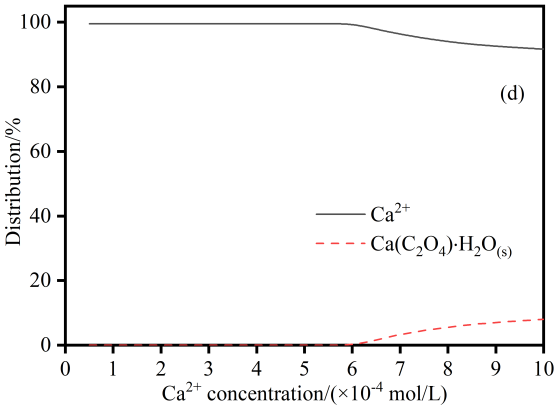

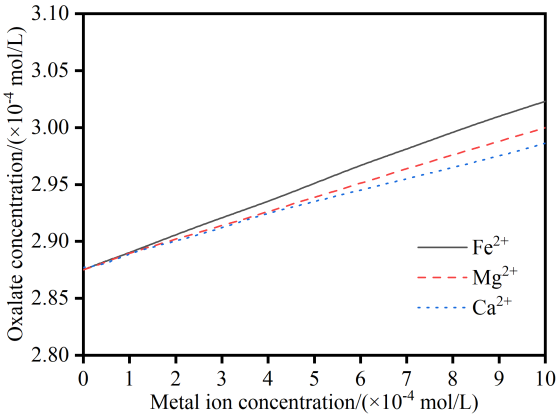

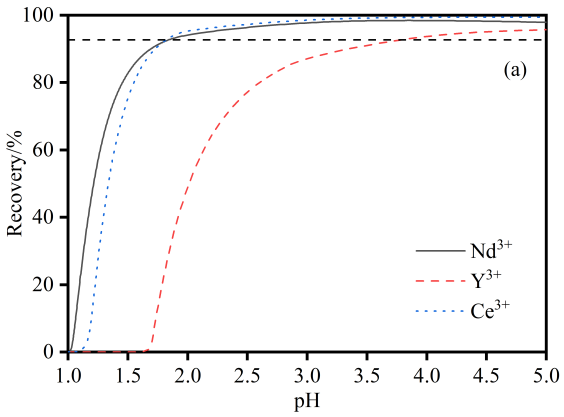

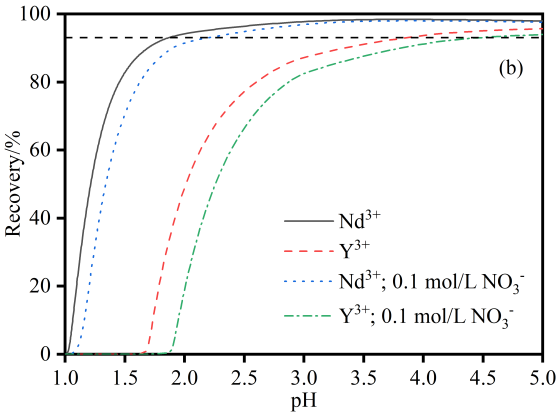

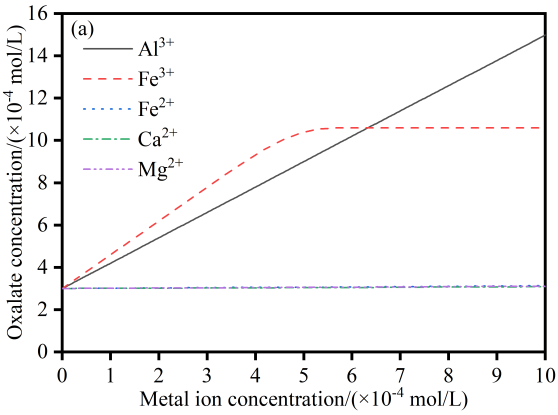

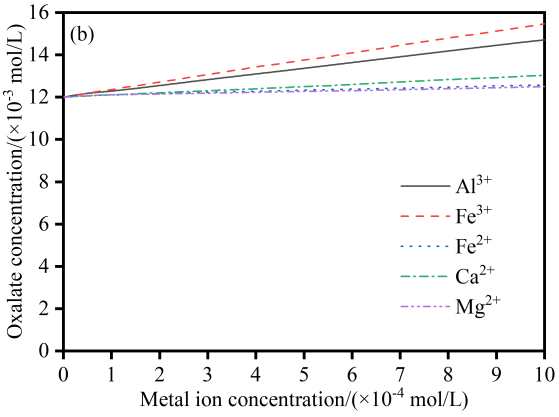

Declaration of interests

☒ The authors declare that they have no known competing financial interests or personal relationships that could have appeared to influence the work reported in this paper.

☐The authors declare the following financial interests/personal relationships which may be considered as potential competing interests: